2 From Extraterrestrial to Terrestrial Applications

G.F.X. Strobl, G. LaRoche, K.-D. Rasch, and G. Hey

2.1 Introduction

In the early 1950s, Bell Laboratories in the USA investigated possible applications of silicon semiconductors in electronics. While improving transistors, Bell scientists Gerald Pearson and Calvin Fuller invented the first silicon solar cell. That first effort was further improved for applications in remote humid locations by Darryl Chapin [1]. The first experiment with silicon yielded an efficiency of 2.3%. Improvements with regard to the dopants, the metallic contacts to the p- and n-side and the application of an antireflection coating led to efficiencies of 4%. In 1954, cells with 6% efficiency could be reliably manufactured.

The first solar battery was presented to the public by Bell Laboratories on April 25, 1954. The battery powered a 21-inch Ferris wheel one day and a solar-powered radio transmitter the next. Technical progress continued and the cell efficiency doubled within two years. Even then, Bell representatives dreamt of a limitless power supply. But this progress could be achieved only with high-purity, single-crystal silicon which was expensive. Thus, a commercial breakthrough was prevented with the exception of some applications by Western Electric to run telephone lines in rural areas. The price at that time was more than $300/W.

Commercialization efforts were undertaken by the National Fabrication Products Company with their chief Scientist Dr. Martin Wolf. But the company did not succeed in bringing the price down and was bought in 1956 by Hoffmann Electronics of El Monte, CA. They developed a 25 W sun-power-to-electricity converter module which no one bought. Its only application was in toys.

At the same time, the U.S. Army Signal Corps investigated possible applications for solar energy converters and found one preferred application: satellites in space! The U.S. Army signal corps was responsible for the design of a solar cell power system for the satellite project Vanguard to be built by the U.S. Navy. They contacted Hoffmann Electronics, and its chief engineer, Eugene Ralph, assembled some of their cells. On St Patrick's Day 1958, Vanguard 1, the first satellite with solar cells aboard, went into orbit. Two months later, SPUTNIK III, also equipped with silicon solar cells, was launched. After six years in orbit, Vanguard 1 was still sending radio messages back to Earth [2].

Despite some early applications on oil platforms, the astronomical price of silicon solar cells limited their use to space. So the onset of the Space Age was the

salvation of the solar cell industry (M. Wolf). From 1958 to 1969 the U.S. government spent more than $50 million on solar cell research and development.

2.2 Solar Cells for Space

Space cells had to be extremely overengineered to withstand the harsh space environment – charged particles, micrometeoroids, hard UV radiation, and temperature extremes due to change of daylight and eclipses all posed challenges. Those challenges required a special design for each satellite, due to individual layout, limited area, storage volume and mass. The solar cell power supplies grew steadily and reached 500 W with the Nimbus Spacecraft in 1964; 1,000 W on the Orbiting Astronomical Observatory in 1966; and 20 kW for the Orbiting Laboratory Skylab in 1972. The upper limit to the size of photovoltaic solar converter arrays in space was given by the capacity of the available launch vehicles. It was found that a high power-to-mass ratio of the solar array was the most important factor which could be increased by improving the solar cell efficiency and/or lowering the solar array mass.

In Germany on August 23, 1962, the "Gesellschaft für Weltraumforschung GfW" was founded to manage and coordinate space activities with the goal of building the first German satellite "AZUR". The satellite's mission was to study cosmic rays and their interference with the Earth's magnetosphere, the northern lights and the time variation of the solar wind due to solar flares. German industry was invited to develop and manufacture the required subsystems and to make the satellite ready for launch. It was launched on November 8, 1969, with a Scout rocket from Cape Canaveral. For this application the solar cell development also took place in Germany at Siemens and Telefunken. These activities benefited from progress made in the U.S. and published in dedicated technical journals and conference proceedings. Importantly, the cells delivered by Telefunken were 2 cm by 2 cm and delivered efficiencies of more than 10%. Moreover, with the introduction of titanium-silver contacts, a technology was developed that became the baseline for all future silicon solar cells for space applications.

Improved understanding of the theory of device operation led to increased efficiency and cost reduction of silicon solar cells (Fig. 2.1 from [2]). But the efficiencies achieved were still far below the theoretical ones. Moreover, theory stated that materials other than Si – like GaAs or CdTe – would give better efficiencies in the Sun spectrum, especially at increased temperatures (Fig. 2.2). Given that Si was the most developed and best understood material, most efforts were directed toward further improvements of Si solar cells. In parallel, other materials like cadmium sulfide, cadmium telluride, and gallium arsenide were investigated but did not achieve better results than silicon. Other thin-film technologies – one based on amorphous silicon and the other on the ternary compound $CuInSe_2$ (CIS) – found applications in electronics and to some extent in power plants.

One advantage of GaAs-based solar cells over Si was their better temperature stability and higher radiation resistance, giving them preference for special

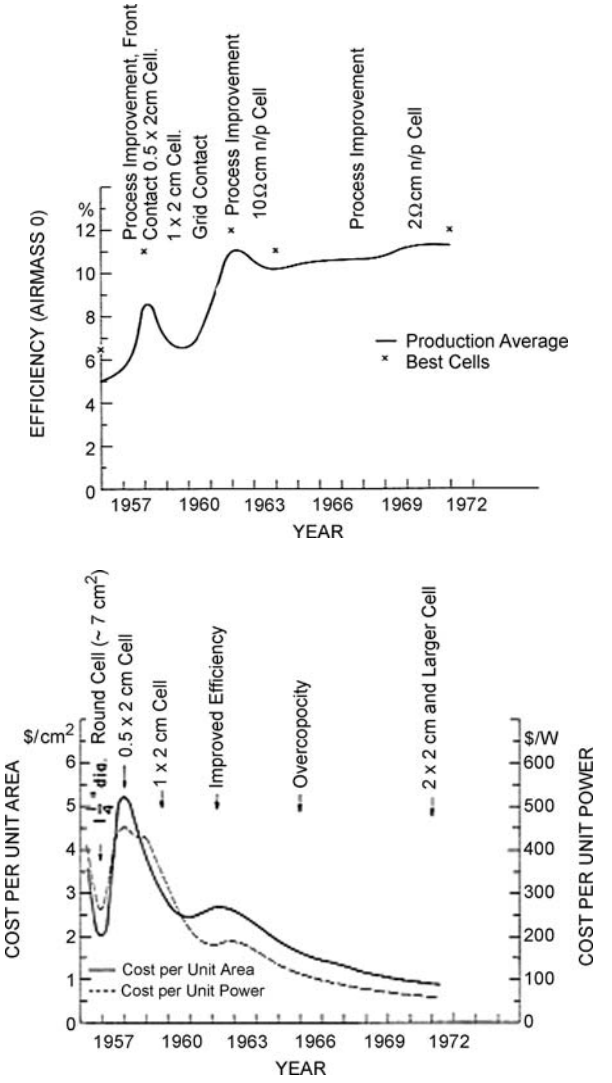

Fig. 2.1. Early historical development of silicon solar cell efficiency (*top*) and cell prices (*bottom*)

applications despite their higher costs. One of the first space applications of the temperature-stable GaAs solar cells took place on the Russian spacecrafts Venera-2 and Venera-3, launched in November 1965 to the "hot" planet Venus. The area of each GaAs solar array fabricated by the Russian Enterprise KVANT for these spacecrafts was 2 m^2. Then, the Russian moon cars were launched in 1970 (Lunokhod-1) and in 1972 (Lunokhod-2) with GaAs 4 m^2 solar arrays in each. The operating temperature of these arrays on the illuminated surface of the Moon was about 130 °C.

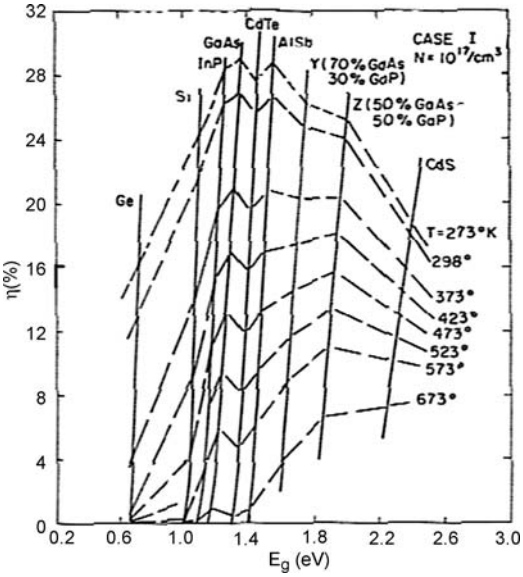

Fig. 2.2. Theoretical efficiencies of different materials at various temperatures (from [3])

The solar arrays demonstrated an efficiency of 11% and have provided the energy supply during the life-time of these moon cars [4].

Further progress was achieved by the development of AlGaAs/GaAs heterostructures, the combination of materials with different energy gaps. Their AM0 efficiency was increased up to 18–19% [5]. A solar array with a total area of 70 m^2 was installed in the Russian space station MIR launched in 1986 (Fig. 2.3). During 15 years in orbit, the array degradation appeared to be lower than 30% under hard operating conditions with appreciable shadowing, the effects of numerous dockings, and a challenging ambient environment of the station.

But GaAs solar cells were more expensive than Si solar cells by a factor 5 to 10, and therefore were used only for special applications. Compared to silicon, the use of GaAs solar cells was considered profitable only if their efficiency would exceed 20%. This was not realistic in the near-term. Therefore, main emphasis was given to further improving the Si technology.

2.3 Closer to the Limit

An analysis of the main loss mechanisms of Si solar cells by M. Wolf [6] yielded the following power-limiting factors:

1. Optical reflection of incident light on the cell surface.
2. Crystal quality limiting quantum efficiency of electron – hole pair production.
3. Loss of excess energy of the majority of absorbed photons necessary to generate electron – hole pairs.

Fig. 2.3. AlGaAs/GaAs solar array on the MIR Space Station (from [4])

4. Low optical absorption coefficient.
5. Recombination of minority carriers on the surfaces, by impurities, dislocations and on the back contact.
6. Reduced barrier height of the junction by the distance of the Fermi levels from the band edges.
7. Loss and leakage currents across the junction and recombination within the depletion layer.
8. Series resistances in the base region and the cell contacts.

The improvement of each factor should bring the real solar cell efficiency closer to the theoretical one. For space applications, the impact of charged particle irradiation had to also be considered. The following main developments were milestones in the improvement of Si solar cells to their present status.

2.3.1 Material Quality

Impurities in the solar cell material generally introduce traps into the crystal. These traps act as recombination centers. An increased density of such centers decreases the minority carrier lifetime and the cell efficiency. On the other hand, silicon must not only be very pure, but it must also be in a single-crystal form with essentially zero defects in the crystal structure. To achieve the required purity the metallurgical grade silicon extracted from silicon dioxide (quartzite) by reduction in large arc furnaces must be further purified by fractional distillation of the condensed volatile

compound $SiHCl_3$ and reduced by hydrogen. This semiconductor grade material is then melted in a crucible with trace levels of the dopant required (normally boron for p-type silicon) and, by means of a seed crystal, large cylindrical single crystals are pulled from the melt (Czochralski process). These so-called boules are sliced up into wafers forming the ingot for the manufacture of solar cells.

Refinements of the above processes improved the wafer quality continuously, allowing higher doping levels which resulted in remarkable efficiency improvements (10 Ω cm versus 2 Ω cm base resistivity). The increase of the crystal diameters from 5.0 cm to more than 12.5 cm allowed the manufacture of large-area solar cells. Though small cells are using the wafer area better (minimum material loss), large area cells were preferred for the subsequent processing steps of cover glassing, cell interconnection and substrate bonding due to cost savings.

2.3.2 Back Surface Reflector (BSR)

The absorption of photons from the incident sunlight depends on the absorption coefficient, which is high for short wavelengths and low for longer wavelengths. Accordingly red and infrared light penetrate deeper into the silicon material and a big portion is scattered or absorbed at the rear side contact. Polishing and coating the rear side with a thin aluminum reflector makes the back contact reflective giving the longer wavelengths a second chance at being absorbed and the energy which is not absorbed is re-emitted through the front surface leading to a reduction in cell absorbance. This is a critical parameter controlling the device's operating temperature.

Such back surface reflectors (BSR) gave a boost to the performance of thin cells and lowered the cell temperature considerably. Thin cells are making solar cells more resistant to charged particle radiation, since minority charge carriers have a higher chance of reaching the pn-junction even in the presence of recombination centers.

2.3.3 Back Surface Field (BSF)

The primary mechanism for the movement of minority carriers toward the pn-junction is the diffusion process. An additional moving mechanism was found to be the drift of minority carriers caused by a built-in electrostatic field arising from gradients of the impurity density. While a positive effect in the diffused region of the cell is found only with a deep junction, which stands against the enhancement of blue response (see violet cell), a drift field is advantageous in the bulk area in order to reduce minority carrier recombination at the rear side. It was found by Wolf [7] that the inclusion of a narrow layer with a drift field in the base region has a marked effect on the performance of the cell and the degradation rates due to nuclear particle radiation. The efficiency of silicon solar cells could be improved by the introduction of a back surface field by up to 17% (e.g., Spectrolab K4700- type compared to Spectrolab K6700-type [8]).

Technologies developed at Telefunken in Germany to form back surface fields consisted of boron diffusion, boron ion implantation and evaporated aluminum paste processes [9]. While the diffusion and implantation processes yielded equal efficiencies at beginning of life, implanted BSF cells showed lower degradation after particle irradiation (end of life EOL condition).

2.3.4 The Violet Cell [10]

Former cells were very limited in the short wavelength region and their diode characteristics were far from ideal. By the existing diffusion process the front regime of a cell consisted of three regions: a shallow region, called the dead layer, with an extremely short lifetime of the minority carriers. This was due to high dopant concentration above the solid solubility limit, a high field region maintained by the impurity profile, and the space charge region. An improvement of the short wavelength response had to eliminate the dead layer, and the recombination states in the space charge region caused by stresses and defects originating in the silicon front surface. Because the dislocation density decreases sharply toward the diffusion front, the dead layer could be eliminated by shallow diffusion. This minimized the total density of dislocations in the diffusion region. This reduction of the emitter thickness caused an increase in the lateral resistance which could be compensated for by increasing the grid lines, thus keeping the solar cell active area constant to avoid shading losses. These improvements in solar cell efficiency increase efficiency by 30% compared with typical commercial cells without changing the degradation behavior under particle irradiation.

2.3.5 Textured Surfaces

Aside from optical coating optimization, another approach to reduce reflection losses is to use textured surfaces. Texturization is achieved by creating a topology of small, densely packed tetrahedral grooves, V-grooves or random pyramids [11] that act as light traps on the solar cell's surface. When light impinges on this textured surface, reflection occurs at such an angle that it is deflected into a new point on the surface. Multiple interactions occur with the silicon, thus reducing the amount of light normally lost through reflection. Together with an antireflection coating the reflection of sunlight can be kept well under 3%, making the cell appear black ("black cell"). The textured surface also provides a reduction in path length to the junction which is most pronounced for longer wavelength light, thereby increasing longer wavelength collection efficiency (an important factor for thin devices) and radiation tolerance. As bulk region diffusion length is reduced by the effects of radiation, the reduced effective path length enables a contoured surface device to maintain more of the lower wavelength response than a comparable smooth cell.

Texturization increases solar absorbance also in the wavelength region not contributing to the carrier generation. To compensate for the resulting higher temperature special infrared (IR) or blue-red-reflecting (BRR) coverglass coatings have been developed.

2.3.6 Contacts

Titanium-silver and nickel-gold with solder on the interconnector pads were used for the solar cell contacts in the early stages [12]. Later, when the welding technique replaced the soldering technique, the solder layer was eliminated and the titanium was protected against electro-corrosion by an intermediate palladium layer. Today the standard contacts consist of Ti/Pd/Ag applied by vacuum evaporation with a subsequent sintering process and photolithographic process for grid forming. A similar process is applied for the rear side with an additional Al-layer serving as BSR.

2.3.7 Bypass Function [13]

Cell breakage or shadowing of solar cells could cause the solar cell to operate in reverse, forming a so-called "hot spot" with temperatures up to 400 °C. This unwanted effect can be avoided by applying a bypass diode in parallel to the cell but in opposite polarity. By special n^+/p^+-doping through the diffusion layer, this bypass diode could be integrated into the cell structure thus saving the additional expense for separate diode application. The application of a bypass function is an indispensable requirement for modern sophisticated GaAs-based multijunction solar cells.

2.3.8 Surface Passivation

Exposed surfaces – such as between gridlines at the top of the cell or the interface between ohmic metal contacts and semiconductor – are generally regions of high carrier recombination velocity. Drift fields prevent the minority carriers from reaching the wrong surface by forming an electric field between highly doped and lightly doped material like for the BSF; these are already effective at reducing recombination velocity.

Another effective method of surface passivation is the growth of a high purity siliconoxide coating in micro-electronic quality. The purer the oxide the higher the passivation effect. This requires special cleaning provisions prior to the growth of the oxide.

A combination of both methods is the local back surface field [14] minimizing recombination at the metallic rear side point contacts while the majority of the cell rear side is passivated by silicon oxide (Fig. 2.9).

2.3.9 Low-Intensity, Low-Temperature Operation

For the ESA deep space mission ROSETTA ASE, the former Telefunken developed a silicon solar cell which did not show power reduction effects under extreme low-intensity, low-temperature (LILT) conditions. The cell possessed all the characteristics for high efficiency, such as a shallow emitter, passivation oxides on front and rear side, textured front side with inverted pyramids, local back surface field and optimum gridline design realized by means of photolithography. The introduction

of a p^+-channel stopper in contact with the emitter provided very good diode characteristics and reverse protection because the n^+/p^+ diode operated like a Zener diode with reverse breakthrough voltages between −6 V and −8 V [15].

2.3.10 Solar Cell Assembly

For space applications, the solar cells use a coverglass for protection against charged particle irradiation and micrometeorites. The cells also require an interconnector to allow solar cell interconnection. The interconnector has to match the solar cell contacts and survive the thermal stresses which can cause multiple gap variations between adjacent cells. Therefore the preferred interconnector material is pure silver, silver coated Kovar or Molybdenum, the latter matching the thermal expansion coefficient of silicon very close. The interconnectors incorporate stress relief measures in order to withstand the mechanical and thermal stresses. In general, resistance welding is applied for the interconnector integration allowing, in connection with a thin interconnector thickness, a 100% coverage of the solar cell by the coverglass.

The coverglass is adhesively bonded to the solar cell front side. It is coated with an anti-reflection coating on the upper side and a UV-reflective coating on the inner side to protect the coverglass adhesive from darkening. Coverglasses with cerium oxide doping absorb the UV and don't need a UV-coating.

Bonding on the substrate, which is in general a carbon-fiber/Al-honeycomb structure with a polyimide foil insulation, is performed with an elastic cement leaving the gaps between the cells free in order to allow the cells undisturbed linear change. The costs for the silicon solar cell assembly and array integration and test are typically three to four times the solar cell costs.

2.3.11 High Efficiency Solar Cells

Figure 2.4a shows the advances in silicon solar cell performance that led to improved current and the voltage. Figure 2.4b shows improvements in electrical power, and Fig. 2.8 shows gains in efficiency. In Fig. 2.4b, 10 mW/cm^2 corresponds to an efficiency of 7.32% at standard air mass zero (AM0) illumination, averaging the sun spectrum and intensity in the air-free space close to the Earth. It should be pointed out that the reference sun spectrum and intensity for terrestrial applications (AM1.5) is different from the AM0 due to absorption and scattering in the atmosphere. This enhances the relative red portion in the spectrum leading to higher silicon solar cell efficiencies.

The production efficiency of a series product with optimized design (Fig. 2.5) achieved 17.5% in the 1980s (Sharp, Telefunken). At that point the development of space solar cells concentrated more and more on Gallium-Arsenide solar cells on Germanium substrate, which were offered by U.S. manufacturers Spectrolab and Tecstar with efficiencies over 19%. These cells were available for a reasonable price and had the potential to realize higher efficiencies. This potential was based on the possibility of using a special epitaxial process to grow several cells monolithically on top of each other, forming a so-called multijunction solar cell [16]. Such cells

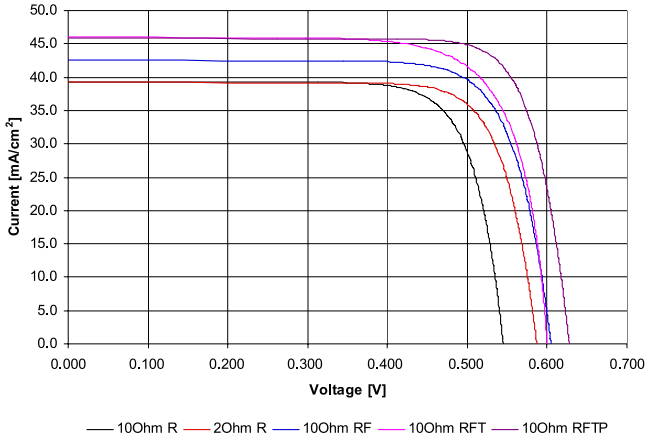

(a) IV-characteristics

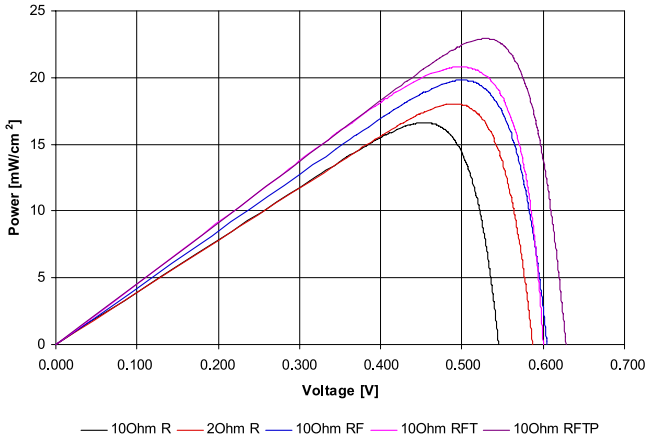

(b) PV-characteristics

Fig. 2.4. Advances in silicon solar cell performance valued at the IV and PV characteristics. Legend: R: back surface reflector; F: back surface field; T: texture; P: passivation

use the sun spectrum much better and operate at much higher voltages. As a consequence, in space applications, silicon solar cells were more and more replaced by GaAs-based solar cells. Nevertheless, the potential of silicon solar cells was not exhausted, and developers found a similar challenging field in terrestrial applications.

Manufacture of multijunction solar cells on the basis of materials from the III/V-groups of the periodic system is possible because the materials can be composed with different band gaps but identical lattice constant. This is necessary for monolithically growing materials on top of each other. Figure 2.6 shows that, for silicon, no suitable crystalline partner can be found limiting the efficiency of silicon solar cells to the monojunction maximum.

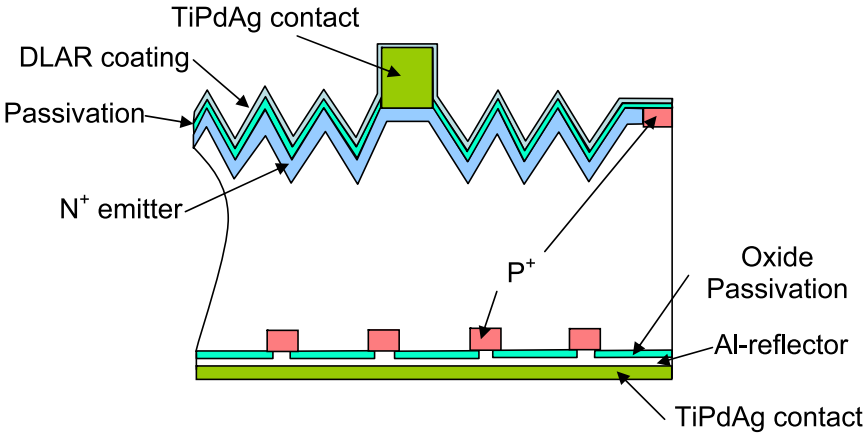

Fig. 2.5. Telefunken 17.5% high-efficiency space solar cell 2wiTHI-ETA®3-ID/ 130

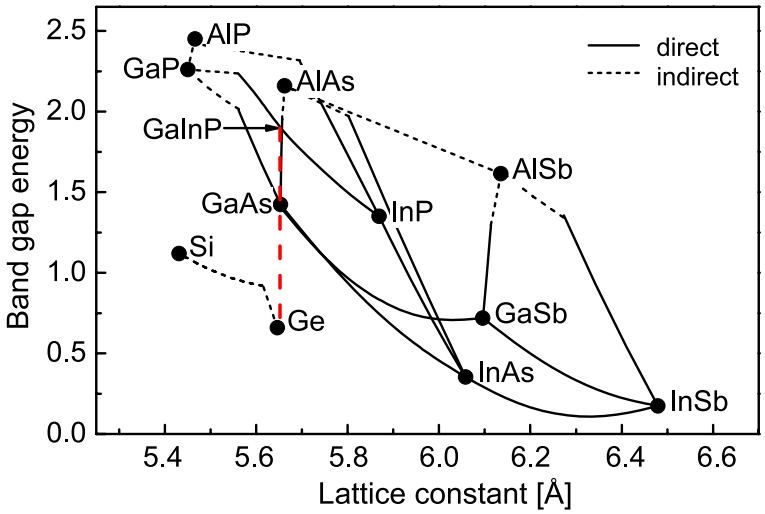

Fig. 2.6. Band gap of some semiconducting materials over their lattice constant. Only materials with same lattice constant like, e.g., Ge – GaAs – GaInP are intermateable

A multijunction solar cell is formed by stacking solar cells of different bandgap on top of one another. With the highest bandgap cell uppermost, light is automatically filtered as it passes through the stack. Each cell absorbs the light it can most efficiently convert, with the rest passing through to underlying cells (Fig. 2.7).

The first monolithic multijunction solar cells came onto the market in middle of the 1990s. These cells featured a dual junction solar cell consisting of a GaInP-top cell and a GaInAs-bottom cell epitaxially grown on a passive Ge-substrate by means of a chemical vapor deposition process using metalorganic precursors (MOCVD).

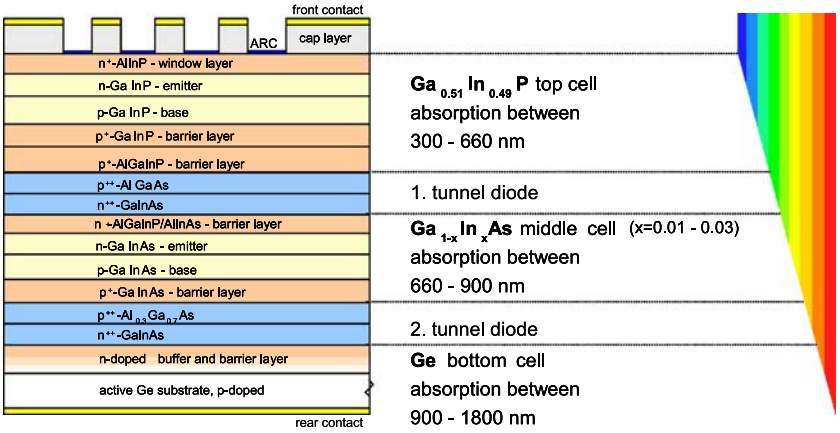

Fig. 2.7. Typical structure of a triple junction solar cell

The improvement compared to a single junction GaAs solar cell was more than 30% and yielded AM0-efficiencies of up to 24%. The first triple junction solar cells were developed at the end of the 1990s and consisted of a GaInP top cell, a GaInAs middle cell and a Ge bottom cell. By continuous improvements in the material, the growth conditions and especially the tunnel diodes separating the subcells from each other, the AM0-efficiency of triple junction cells has been improved from 25% in 2002 to 28.5% in 2006 (see Fig. 2.8). By optimizing the subcell design, the sensitivity to particle irradiation is only half that of silicon solar cells [17, 18]. Both high efficiency and high radiation hardness make the GaAs-based multijunction solar cells ideal for powering spacecrafts. But the price, which is more than five times that of a high-efficiency silicon solar cell (due to the sophisticated cell structure reflected in Fig. 2.7) limits terrestrial applications to concentrating systems.

Terrestrial applications started by adapting the technology developed for space as far as feasible. The developers of terrestrial photovoltaics did not have to consider the harsh space environment impacts and the mass requirements imposed on the design of space grade solar generators. Instead, the modules required encapsulation to protect the metallic cell contacts and interconnectors from corrosion and from mechanical damage caused by handling, hail, birds, and objects dropped or thrown on them. Additional requirements were UV stability, tolerance against terrestrial temperature extremes, abrasion hardness and self-cleaning ability. These requirements were met by a substrate consisting of aluminum, steel, epoxy board or window glass, a glass window, and as an encapsulant silicone adhesive or, alternatively, polyvinyl butyral (PVB) or ethylene/vinyl acetate (EVA).

But these solutions could not be realized in very large quantities at costs that allow solar-generated electricity to compete with wholesale electricity prices. To do so required not only low-cost approaches and low energy consumption during cell fabrication, but also high energy conversion efficiency to offset unavoidable area-related material and installation costs.

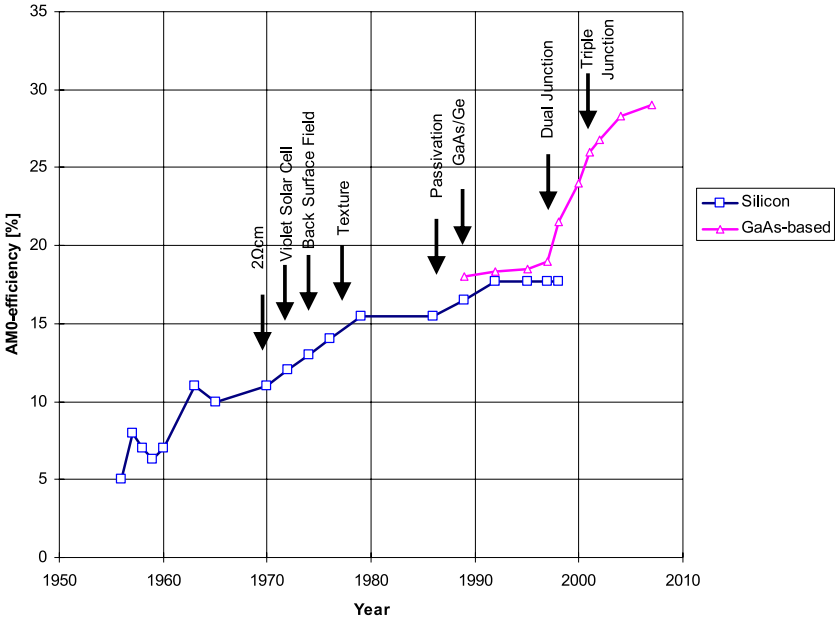

Fig. 2.8. Development of AM0-efficiency for space solar cells

To further improve the silicon solar cell efficiency, the following features have been introduced step-by-step:

- Highly doped bulk material (1 Ω cm base resistivity compared to 2–10 Ω cm for space solar cells).
- Use of float zone (FZ) silicon crystals instead of crucible grown (CZ). Due to the absence of oxygen in the molten silicon during the FZ process, there are no effects of thermal donors or oxygen precipitates. This produces a silicon wafer that has extremely stable resistivity performance and high carrier lifetimes. For space applications FZ material degrades more under combined particle/UV-radiation than CZ.
- Optimized emitter. In order to gain the full benefit of improved emitter surface passivation on cell performance, it is necessary to tailor the emitter doping profile so that the emitter is lightly doped between the gridlines, yet heavily doped under them.
- Shorter and narrower grid lines allow higher fill factors. Another approach for an improved fill factor is a shingled array design. Cells overlap in the module and the cell busbar area is shaded by the following row of cells. This allows a wide busbar design.
- Laser-grooved grid contacts followed by a second enhanced phosphorous diffusion producing selective doping in the contact areas.

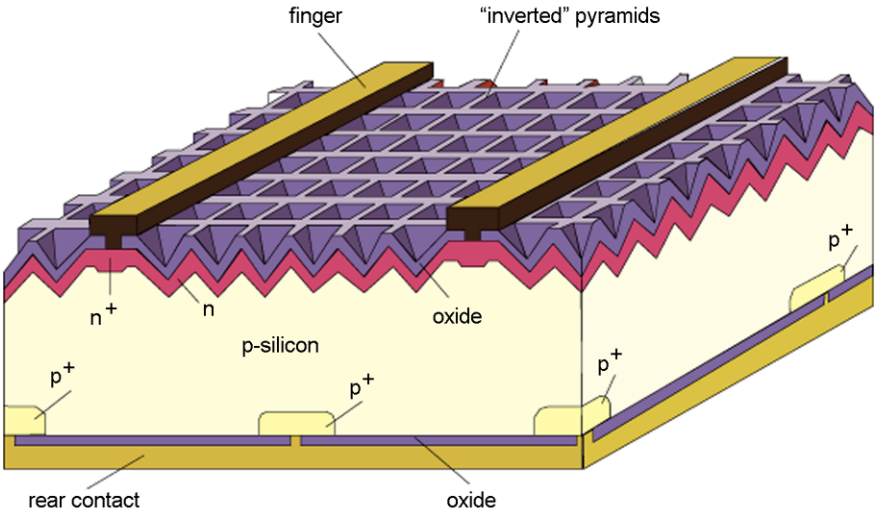

Fig. 2.9. Schematic of a PERL silicon solar cell (www.udel.edu/igert/pvcdrom)

A cell incorporating all of these improvements – in addition to the achievements of the space industry – is the passivated emitter with rear locally diffused (PERL) cell. This cell was developed by the University of New South Wales (Australia) (Fig. 2.9 and [19, 20]). It uses micro-electronic techniques to produce cells with efficiencies approaching 25% under the standard terrestrial AM1.5 spectrum. The passivated emitter refers to the high-quality oxide at the front surface that significantly lowers the number of carriers recombining at the surface. The rear is locally diffused only at the metal contacts to minimize recombination while maintaining good electrical contact.

Such extremely high-efficiency solar cells are very suitable for special applications, such as solar car racing, research and other applications where efficiency is the prime consideration. They are not a cost-competitive solution to most domestic and commercial solar cell applications. Achieving 23–25% efficiency, their price at ca. $400 U.S./W is about 100 times the cost of a standard commercial solar cell. They are cost prohibitive even for space applications.

The 1990 World Solar Challenge (WSC_solar-powered car race was won by "The Spirit of Biel" from the Engineering University of Biel, in Switzerland. Biel's winning time was 46 hours and eight minutes (65.3 ave. kmph). Biel's array was composed of laser-grooved aerospace cells that were connected by overlapping them in shingle style. The combination of high-efficiency cells with a high packing density (97.5%) resulted in an impressive 170 watts per square meter. The sleek, colorful, 182 kg solar racing car was clocked at 101 km/h during qualification trials and cruised at 72.4 km/h under mid-day sun [21].

2.4 Cost Reduction Measures

The efforts toward cost reduction had to consider design, materials and processes while keeping cell performance as high as possible. The most important parameter became the power-to-cost ratio replacing the power-to-weight ratio applicable for space solar generators. Compared with the highly sophisticated space technology, the following simplifications have been achieved step-by-step.

The major portion of the material costs is the expensive purification of the raw silicon and the single-crystal growing processes. Therefore numerous efforts have been undertaken to create basic material using less-pure silicon and a lower degree of crystalline perfection than the semiconductor-grade silicon.

2.4.1 Silicon Production

Alternative processes have been developed that, at a fraction of the cost of conventional semiconductor-grade silicon, create cells capable of adequate performance. The most common process applies the so-called fluid bed principle, using Trichlorosilane Cl_3HSi as the charge material which is then transferred into Monosilane SiH_4. From this the solar-grade silicon is extracted by cracking. This process is capable of reducing the costs required for semiconductor-grade material by 70%.

2.4.2 Bulk Material

A lot of material is lost by cutting the wafers into rectangular shapes. This waste of material can be avoided by using circular cells for the module assembly at the cost of low packing density. Waste can also be reduced by growing the ingots in square cross-sections to begin with. This can be achieved by casting silicon into boules or bricks. This process saves money compared to the CZ single-crystal growth technology but produces polycrystalline material instead of monocrystalline [22]. It has been demonstrated that a cell made of cast silicon can produce 12% to 14% efficiency and cost about 60% of a typical CZ cell. However, the slicing process is still necessary by which 50% of the material is lost.

A process that avoids material loss by slicing is the edge-defined, film-fed growth (EFG) of silicon [23]. This process consists of a slotted die of carbon or quartz which is partly dipped into molten silicon. The liquid silicon wets the die and is attracted into the slot by capillary action, forming a ribbon with the cross-section of the slot. Ten-cm wide ribbons at speeds up to 4 cm/min. were successfully grown in 1980 [24]. The process has been optimized by SCHOTT Solar (formerly RWE Solar), growing polycrystalline ribbons with a width of 15 cm at a growth speed of more than 10 cm/min. applying octagonally shaped dies.

2.4.3 Cell Contacts

Alternative developments replacing the expensive evaporation process were nickel plating followed by solder dipping and screen printing of metal pastes. Using the

latter method, thin layers of a paste with fine-grained metal powder are printed on the cell surface by silkscreen technique and fired afterwards in a continuous sintering furnace under inert atmosphere. Fine glass particles dispersed in the paste act as binders for the metal powder after firing. This process reduced costs by replacing the expensive, high-purity titanium – silver with an aluminum – silver mix and the discontinuous evaporation procedure by a continuous process. On the rear side, the addition of aluminum increases the doping level in the surface region with the alloy forming a back surface field. There are several disadvantages to this technology, including a restricted width of the gridlines, a high contact resistance between paste and silicon, and low conductivity of the sintered material.

These disadvantages were extensively reduced by employing a buried contact design. Grooves, cut into the top surface emitter by laser scribing, mechanical or chemical approaches, provide for increased contact area and grid finger cross-section. The metal application is either by screen printing or is electroless by immersing the wafers in a plating solution. Grooved contacts give a 30% performance advantage over screen printed cells without grooves.

2.4.4 Encapsulation

The encapsulation of the modules has to guarantee long life operation under extreme weather conditions. For the transparent front side, safety glass is commonly used; its thickness results from a trade-off between material cost savings and additional costs due to increased breakage rate. The rear side is made either of glass, like the front side, or of a weather- and waterproof foil back. The cells are embedded in silicone or in ethylene vinyl acetate (EVA). For edge protection and mounting the assembly is firmly bordered with a sturdy, fully closed aluminum frame. An automated production line with high throughput ensures consistent product quality and low costs.

2.5 Concentrating Systems – A New Opportunity for High Efficiency Space Solar Cells

The power-to-weight ratio of a terrestrial module is typically more than 10 W/kg compared to 100 W/kg for a typical space solar array. Launch costs in the range of 20,000 €/kg justify the application of highly sophisticated technology for space.

Nevertheless, high-efficiency space grade solar cells have a good chance of entering the terrestrial market. The primary impediment to direct application is the high price. But this can be drastically reduced by operating the solar cells in a concentrated system. This has two advantages: On the one hand, the cell size is reduced approximately proportional to the concentration factor; on the other hand, the efficiency is increased by a factor proportional to the logarithm of the concentration. These facts have prompted a resurgence of research in multijunction cells and commercial interest in concentrator III–V photovoltaics. Of particular interest are high

Fig. 2.10. 190 kWp power station by Solar Systems [27]

concentration systems. A record 40.7% efficiency at 240 suns was reported at the Madrid Conference in 2007 [25].

Over more than 30 years many research groups were engaged in developing concentrator photovoltaic systems (CPV). In the first concentrator modules and installations, large-area mirrors (0.5–1 m in diameter) focused the sunlight on cells of several square centimeters in area. Cooling by water or by means of thermal pipes was necessary [26]. Several reliable and efficient CPV power stations have been demonstrated, e.g., by Solar Systems in Australia (Fig. 2.10 and [27]). For this system, a new triple junction receiver was developed to replace the current silicon point-contact solar cells. The new receiver technology is based on high-efficiency ($>35\%$) concentrator triple junction solar cells from Spectrolab, resulting in system power and energy performance improvement of more than 50% compared to the silicon cells. This is also due to the fact that multijunction cells exhibit lower ohmic losses because they operate at lower currents.

Appearance of the technology accessible for Fresnel lens fabrication has determined revision of the photovoltaic module design. Solar cells could be placed behind the concentrators in this case. The module housing could serve as a protector from the environment and provided for cooling by thermal conductivity. Since the Fresnel lenses had smaller dimensions (25×25 cm^2), the photocell dimensions were also decreased down to less than 1 cm^2.

In the late 1980s, the Ioffe Physico-Technical Institute, St. Petersburg [28] proposed the concept of a radical decrease in the concentrator dimensions while retaining a high sunlight concentration ratio. The first experimental modules of such a

Fig. 2.11. Array of the Ioffe full-size concentrator modules with small aperture area Fresnel lenses

type consisted of a panel of lenses, each of 1×1 or 2×2 cm^2, focusing radiation on AlGaAs/GaAs cells of submillimeter size. At that time, the main advantages of a module with small-aperture area concentrators were: the requirements imposed on the capability of heat-sinking material to conduct heat, on its thermal expansion coefficient and on its thickness are essentially relieved. The focal distance of such lenses appeared to be comparable with the structural thickness of the conventional modules without concentrators.

The team at the Ioffe Institute has developed concentrator modules [29] in which Fresnel lenses are arranged on a common superstrate to form a panel of 12×12 lenses. Cells as small as 2×2 mm^2 and 1.7 mm, in a designated area diameter and operating at a mean concentration ratio of about 700×, are used (Fig. 2.11). The lens profile was optimized, taking into account the refraction index of the lens material and its dependence on wavelength, focal distance, receiver diameter, sun illumination spectrum, and the sensitivity spectra of the subcells in a multijunction cell. The lens structure consists of a sheet of silicate glass and refracting microprisms formed of transparent silicone on the inner side of the glass. The microprisms themselves are formed by polymerization of the silicone compound directly on the glass sheet with the use of a negatively profiled mold. The advantages of this concentrator technology are based on the high UV stability of silicone, its excellent resistance to thermal shocks and high/low temperatures, good adhesive properties in a stack with silicate glass, simplicity and very high accuracy of the formation method. The accuracy of cell position is of great importance because each cell must be placed in the center of the focal spot of a corresponding lens. This accuracy has to be about 100 μm, which is realized by using automatic processes and standard electronic industry machines.

The overall module outdoor conversion efficiency as high as 24.6% was measured on a 2×4 lenses module. But the outdoor efficiency could exceed 28% at

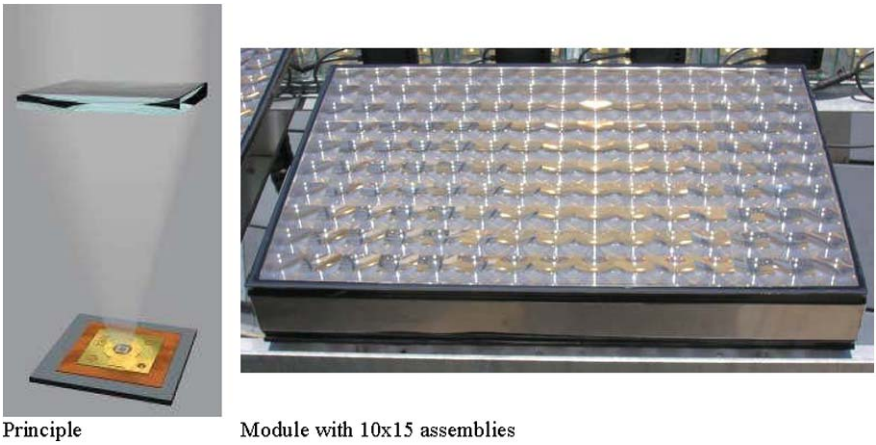

Fig. 2.12. FLATCON®-module Technology [31]

lower ambient temperature, or at the use of the cells with indoor efficiencies in the range of 39–40% instead of used ones with 32.34%.

Concentrix Solar, Germany, also uses high-efficiency triple junction solar cells in their FLATCON®-modules [30, 31]. Figure 2.12 shows the principle of the FLATCON technology and a photo of a module consisting of 150 Fresnel lenses made of embossed silicone on a $4 \times 4\,\mathrm{cm}^2$ glass plate equipped with circular triple junction cells with an active area diameter of 2.3 mm and a grid design optimized for the inhomogeneous illumination under the Fresnel lens. Under standard test conditions the efficiency is 33.0% at 300–500 suns. Typical operating module efficiency is 25.5%.

Most of the progress in solar cell development has been made for space use to the benefit of terrestrial applications. However, some of the technological improvements are starting to flow the other way, with discussion of solar cells made from copper-indiumdiselenide (CIS) material. This thin-film technology is very resistant to charged particle degradation and could be considered for space missions exposed to extremely difficult charged particle environment, e.g. those near the Jupiter moon Europa.

References

1. J. Perlin, *From Space to Earth: the Story of Solar Electricity, AATEC Publications* (Ann Arbor, Michigan, 1999). ISBN 0-937948-14-4
2. M. Wolf, Historical development of solar cells, in *Proc. 25th Power Sources Symposium*, 23–25 May 1972
3. J.J. Wysocki, P. Rappaport, Effect of temperature on photovoltaic solar energy conversion. J. Appl. Phys. **31** (1960)

4. Z.I. Alferov, V.M. Andreev, V.D. Rumyantsev, *III–V solar cells and concentrator arrays*, Ioffe Physico-Technical Institute, 26 Polytechnicheskaya str., St. Petersburg 194021, Russia
5. V.M. Andreev, V.R. Larionov, V.D. Rumyantsev, O.M. Fedorova, Sh.Sh. Shamukhamedov, P AlGaAs – pGaAs – nGaAs solar cells with efficiencies of 19% at AM0 and 24% at AM1.5. Sov. Tech. Phys. Lett. **9**(10), 537–538 (1983)
6. M. Wolf, A new look at silicon solar cell performance. Energy Convers. **11** (1971)
7. M. Wolf, Drift fields in photovoltaic solar energy converter cells, in *Proc. IEEE*, vol. 51, May 1963
8. Spectrolab Inc. Spectrolab production solar cell design data, 10 August 1981
9. G. Strobl et al., Experiences with implanted BSF solar cells, in *Proc. 4th European Symposium "Solar Generators in Space" Cannes*, 18–20 Sept. 1984 (ESA SP-210)
10. J. Lindmayer, J.F. Allison, The violet cell: an improved silicon solar cell, in *Ninth IEEE Photovoltaic Specialists Conference*, Silver Spring, Md., 2–4 May 1972
11. C.R. Baraona, H.W. Brandhorst, V grooved silicon solar cells, in *Proceedings of 11th Photovoltaic Specialists Conference*, 1975
12. P. Iles, Present state of solar cell production, in *Proc. 5th PVSC, NASA-GSFC*, Greenbelt, MD, 1965
13. T. Hisamatsu, H. Washio et al., Reverse bias characteristics of modules made of solar cells with and without integrated bypass function (IBF), in *Proc. 25th PVSC*, Washington, D.C., 13–17 May 1996
14. AZUR Patent DE 3815512C2
15. G. Strobl, H. Fiebrich, Production experience with LILT silicon solar cells for ROSETTA qualification, in *Proc. of 2nd WCPSEC*, Vienna, July 6–10 1998
16. B. Beaumont, J.P. Contour, P. Gibart, J.C. Guillaume, C. Vèrié, Conversion photovoltaique à haut rendement: le projet quadrispectral, in *Proc. 4th Europ. Symp. "Photovoltaic Generators in Space"*, Cannes, 18–20 Sept. 1984 (ESA – SP-210 Nov. 1984)
17. M. Meusel et al., Development status of European multi-junction space solar cells with high radiation hardness, in *Proc. 20th EPSEC*, Barcelona, 2005
18. G. Strobl et al., European roadmap of multijunction solar cells and qualification status, in *IEEE 4th World Conference on Photovoltaic Energy Conversion*, Waikoloa, Hawaii, 7–12 May 2006
19. J. Zhao, A. Wang, E. Abbaspour-Sani, F. Yun, M.A. Green, 22.3% efficient silicon solar cell module, in *25th PVSC*, Washington, DC, 13–17 May 1996
20. M.A. Green, *Silicon Solar Cells – Advanced Principles & Practice* (Sydney, 1996)
21. R.J. King, Recent car technology developments including Australian world solar challenge results, in *Proc. of 22nd IEEE PVSC*, 1991
22. K. Roy, K.-D. Rasch, H. Fischer, Growth structure of cast silicon and related photovoltaic properties of solar cells, in *Proc. 14th PVSC*, San Diego, CA, 1980
23. H.E. Bates, D.N. Jewett, V.E. White, Growth of silicon ribbon by edge defined, film-fed growth, in *Proc. 10th IEEE PVSC*, 13–15 Nov. 1973
24. J.P. Kalejs, B.H. Mackintosh, E.M. Sachs, F.V. Wald, Progress in the growth of wide silicon ribbons by the EFG technique at high speed using multiple growth stations, in *Proc. 14th IEEE PVSC*, San Diego, CA, 1980
25. R.R. King et al., Metamorphic concentrator solar cells with over 40% conversion efficiency, ECSC-4, in *4th International Conference on Solar Concentrators*, Madrid, 12–16 March 2007
26. Z.I. Alferov, V.M. Andreev, Kh.K. Aripov, V.R. Larionov, V.D. Rumyantsev, Pattern of autonomal solar installation with heterostructure solar cells and concentrators. Geliotechnica **2**, 3–6 (1981). Appl. Solar Energy **2** (1981)

27. P.J. Verlinden et al., Performance and reliability of multijunction III–V modules for concentrating dish and central receiver applications, in *IEEE 4th World Conference on Photovoltaic Energy Conversion*, Waikoloa, Hawaii, 7–12 May 2006
28. V.M. Andreev, V.R. Larionov, V.D. Rumyantsev, M.Z. Shvarts, High-efficiency solar concentrating GaAs-AlGaAs modules with small-size lens units, in *11th European Photovoltaic Solar Energy Conference and Exhibition – Book of Abstracts; abstract No. 1A. 15*, Montreux, Switzerland, 12–16 October 1992
29. V.M. Andreev, E.A. Ionova, V.D. Rumyantsev, N.A. Sadchikov, M.Z. Shvarts, Concentrator PV modules of "all-glass" design with modified structure, in *Proceedings of 3rd World Conference on Photovoltaic Energy Conversion 3P-C3-72*, 2003
30. A.W. Bett et al., High-concentration PV using III–V solar cells, in *2006 IEEE 4th World Conference on Photovoltaic Energy Conversion*, Waikoloa, Hawaii, on 7–12 May 2006
31. H. Lerchenmüller et al., From FLATCON® pilot systems to the first power plant, ECSC-4, in *4th International Conference on Solar Concentrators*, Madrid, 12–16 March 2007